Application of Matrix Converters in Photovoltaic Systems

Carlos José Domingos dos Santos
Instituto Superior Técnico

Abstract — The current fuel crisis and environmental issues are boosting the role of renewable energies all around the world. Their growing importance makes it necessary to find ways to enhance the current solutions' performance or find new, more attractive ones [1]. This paper proposes an alternative to the common power converters used in photovoltaic systems.

The matrix converter has already been studied as a good solution on other renewable energy systems, such as wind energy [2]. Also many studies have already been made for DC/AC applications with successful results [3] [4] [5] [6], which suggest that photovoltaic applications are viable.

Simulation tests show the performance of the proposed topology.

Key Words: Matrix Converter; Photovoltaic Energy; MPPT; Unitary Power Factor Control

1 Introduction

Being the Sun the highest power source known, photovoltaic energy is thought as being of high potential although the technology of the systems currently used offer limited efficiency (a maximum of 24% in laboratory environment, 15% in field applications) [1] [7]. Some of the efficiency lost is due to the converters currently used and the control systems to maximize the power input of the solar panel [1].

Matrix converters are a rather young technology, although studies have begun around the 70's, but the potential of this topology is well known in the scientific community. Amongst the advantages there is the unit power factor and the reduction on size and weight due to the absence of large reactive components [2] [5]. Also the waveform and frequency from both sides of the converter are completely independent [3].

Although these advantages this technology is still mainly experimental, with very little market exploitation, due to their high prices [2].

2 Photovoltaic System

The photovoltaic system is composed of cells, made of silicon, that form modules and panels for bigger power generation.

The cells, modules or panels can be represented by an equivalent electric circuit, as shown on Fig. 1 where I_S represents the electric current generated by the solar radiation, I_D is the diode current, I and V are the output current ant voltage.

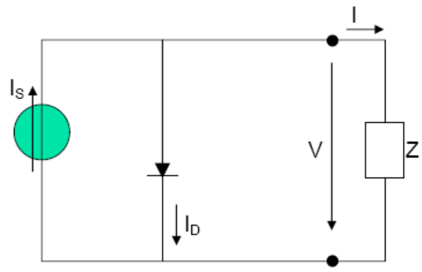

Fig. 1 – Equivalent electric circuit of a photovoltaic system [7]

The diode current, I_D, is given by (1) where I_0 is the dark current and m is the diode ideality factor, V_T is the thermal potential.

$$I_D = I_0\left(e^{\frac{V}{mV_T}} - 1\right) \quad (1)$$

Substituting I_D for (1), the output current, I, is equal to (2).

$$I = I_S - I_0\left(e^{\frac{V}{mV_T}} - 1\right) \quad (2)$$

This gives us the current-voltage relation, I-V, of the photovoltaic system. The equation (2) is the mathematical model of the photovoltaic system.

The I-V relation of a typical photovoltaic cell is shown on Fig. 2. This would be equivalent to a model or panel relation, on a smaller scale.

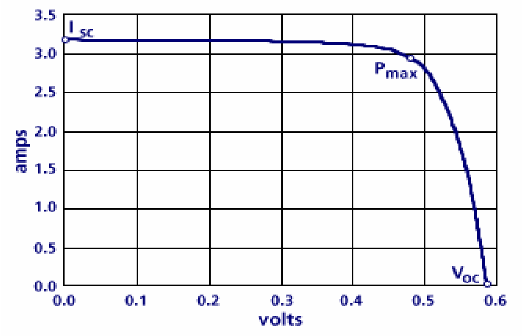

Fig. 2 – Typical I-V relation of a photovoltaic cell [7]

The voltage and current outputs of a photovoltaic panel depend on temperature and solar radiation. Temperature affects both I_0 and V_T values and solar radiation affects I_S.

Modules and panels producers often indicate technical data, like power, voltage and current for some reference temperature, T^r (298,16ºK), and solar radiation, G^r (1000W/m^2), values [7].

The relation between V_T and temperature, T, is given by (3). With K being the Boltzmann's constant (1,3805x10^{-23} Nm/ºK), q is the electron charge (1,6x10^{-19} C) and T is the temperature (ºK). For T^r, V_T is equal to V_T^r.

$$V_T = \frac{KT}{q} \tag{3}$$

I_0 also varies with the temperature, according to (4) where ε is the band gap for silicon (1,10eV) and I_0^r is the value in reference conditions [1] [7].

$$I_0 = I_0^r \left(\frac{T}{T^r} \right)^3 e^{\frac{\varepsilon}{m}\left(\frac{1}{V_T^r} - \frac{1}{V_T} \right)} \tag{4}$$

For modules and panels, m will not be the original value, as it depends on the number and type of cells the module is made off, and the number of modules if we are referring to a panel.

With (3) and (4) it is now possible to understand the effect of temperature variation on the photovoltaic system, as illustrated by Fig. 3.

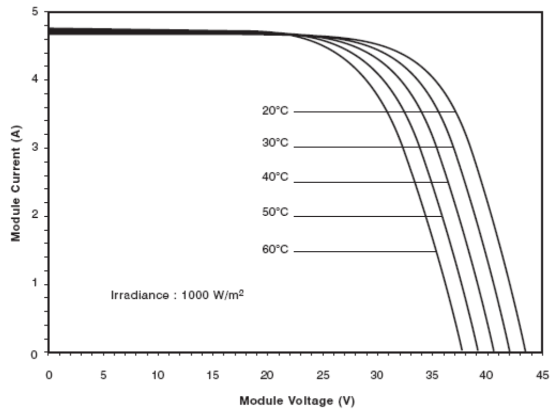

Fig. 3 – Temperature variation effect on the I-V relation [7]

The relation between I_S and solar radiation, G, is given by (5) where I_S^r is the value of I_S in reference conditions [7].

$$I_S = I_S^r \frac{G}{G^r} \tag{5}$$

Equation (5) means that variations on solar radiation will also affect the output of the photovoltaic system, as shown on Fig. 4.

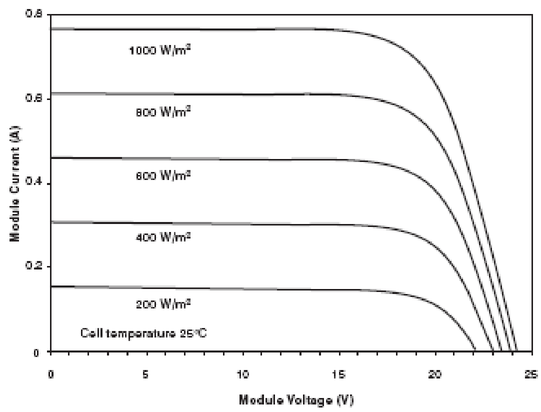

Fig. 4 – Solar radiation variation effect on the I-V relation [7]

Knowing the behaviour of the photovoltaic system we know what to expect from the simulation model, which will be important to analyse the simulation results.

3 Matrix Converter

3.1 Matrix converter topology

The matrix converter is a direct frequency converter, able to perform AC/AC, DC/AC and DC/DC convertions. It uses bi-directional switches, with a switch connected between each input terminal to each output terminal. This arrangement allows reverse power flow through the converter [5].

The AC/AC and DC/AC matrix converter structure is shown in Fig. 5.

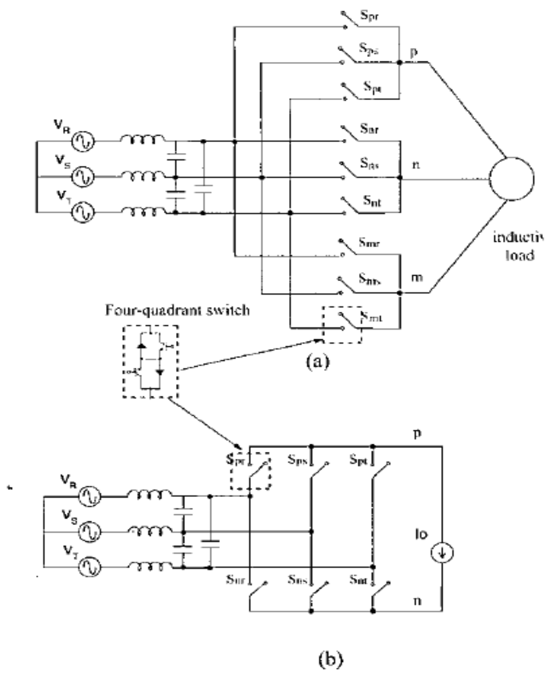

Fig. 5 – Basic topology of a AC/AC matrix converter (a) and reduced DC/AC matrix converter (b) [5]

An important requirement in power converters is isolation between source and load. The previous converting solutions used reactive components that make the converter a bulky and heavy equipment. The solution on matrix converters is the use of filters [5]. In this paper a three-phase RLC filter was used for the AC circuit and a RL filter was used for the DC circuit.

3.2 DC/AC matrix converter model

To guarantee the matrix converter correct functioning there are certain topologic restrictions we need to attend. Having Fig. 5 as reference, there should always be one switch on the upper side (S_p) and one on the lower side (S_n) of the converter, turned on. But there can be no more that one because it would create a short-circuit between two AC phases.

Designating each switch as S_{ij}, where i and j define the output/input phase of the converter. If the switch is off then S_{ij}=0, if the switch is on then S_{ij}=1.

The matrix **S** (6) defines the estate of each switch and is part of the reason this converters are called matrix converters.

$$\mathbf{S} = \begin{bmatrix} S_{11} & S_{12} & S_{13} \\ S_{21} & S_{22} & S_{23} \end{bmatrix} \tag{6}$$

The relation between DC and AC voltage is (7).

$$\begin{bmatrix} V_D \\ V_C \end{bmatrix} = \mathbf{S} \begin{bmatrix} v_a \\ v_b \\ v_c \end{bmatrix} \tag{7}$$

And the relation for the currents is (8).

$$\begin{bmatrix} i_a \\ i_b \\ i_c \end{bmatrix} = \mathbf{S}^T \times I_{DC} \tag{8}$$

With (6), (7), (8) and the topologic restrictions in mind we can build Table 1.

Table 1 – Matrix converter states, voltage and current relations

nº	S_{11}	S_{12}	S_{13}	S_{21}	S_{22}	S_{23}	V_D	V_C	V_{DC}	I_a	I_b	I_c
1	1	0	0	0	1	0	v_a	v_b	v_{ab}	I_{DC}	$-I_{DC}$	0
2	0	1	0	1	0	0	v_b	v_a	$-v_{ab}$	$-I_{DC}$	I_{DC}	0
3	0	1	0	0	0	1	v_b	v_c	v_{bc}	0	I_{DC}	$-I_{DC}$
4	0	0	1	0	1	0	v_c	v_b	$-v_{bc}$	0	$-I_{DC}$	I_{DC}
5	1	0	0	0	0	1	v_a	v_c	$-v_{ca}$	$-I_{DC}$	0	I_{DC}
6	0	0	1	1	0	0	v_c	v_a	v_{ca}	I_{DC}	0	$-I_{DC}$
7	1	0	0	1	0	0	v_a	v_a	0	0	0	0
8	0	1	0	0	1	0	v_b	v_b	0	0	0	0
9	0	0	1	0	0	1	v_c	v_c	0	0	0	0

This table will be the base for the matrix converter system.

4 Control

Nowadays the most used control technique is the space vector modulation. This technique allows a space representation of the 9 states of the DC/AC converter.

The Concordia transformation is used to convert the three-phase voltage system in an equivalent voltage system (9), [2].

$$\mathbf{C} = \sqrt{\frac{2}{3}} \begin{bmatrix} 1 & 0 & \frac{1}{\sqrt{2}} \\ -\frac{1}{2} & \frac{\sqrt{3}}{2} & \frac{1}{\sqrt{2}} \\ -\frac{1}{2} & -\frac{\sqrt{3}}{2} & \frac{1}{\sqrt{2}} \end{bmatrix} \tag{9}$$

The equivalent voltage system is defined by (10), [2].

$$\begin{bmatrix} v_\alpha \\ v_\beta \\ v_0 \end{bmatrix} = \mathbf{C}^T \begin{bmatrix} v_{ab} \\ v_{bc} \\ v_{ca} \end{bmatrix}$$
(10)

The homopolar voltage, v_0, is null. We can represent v_α and v_β by their module and argument as shown on Table 2, which allows us to represent them as vectors on the α-β plane.

Table 2 – Module and argument of each vector on the α-β plane

Estado	V_0	δ_0
1	v_{ab}	-30º
2	$-v_{ab}$	-30º
3	v_{bc}	90º
4	$-v_{bc}$	90º
5	$-v_{ca}$	30º
6	v_{ca}	30º
7	0	-
8	0	-
9	0	-

Fig. 6 represents the space vectors in Table 2 on the α-β plane.

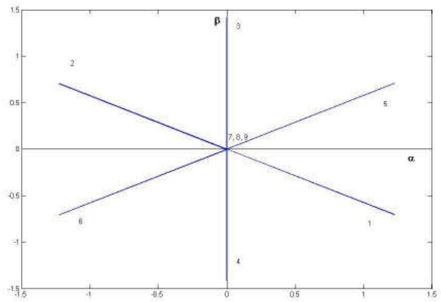

Fig. 6 – Space vectors on the α-β plane

The control of the matrix converter is made by selecting the vector that instantly best suits the system requirements.

There are two control specifications on the application of the matrix converter in photovoltaic systems.

- Maximum photovoltaic panel power output control, better known as MPPT – Maximum Power Point Tracker;
- Unitary power factor control on the input AC currents.

To satisfy both specifications we need two independent control systems, whose signals can be combined in a single control signal.

4.1 MPPT – Maximum Power Point Tracker

MPPTs are common on photovoltaic systems. The typical MPPTs are usually hard processing units (computers or microprocessors). These are expensive equipments and usually introduce delays on the system.

In this paper a different type of MPPT is used, already introduced in some other works. This type is based on power differentiation.

We know the relation between power, voltage and current (11).

$$P = VI$$
(11)

If we choose to make the derivative of power, P, in respect to the current, I, we have (12), [1].

$$\frac{dP}{dI} = 0 \Leftrightarrow V + I\frac{dV}{dI} = 0 \Leftrightarrow V = -I\frac{dV}{dI}$$
(12)

If we consider that voltage and current variations are small on small time intervals, which is reasonable since solar radiation and temperature varies slowly in small time intervals, then (12) is approximately equal to (13), [1].

$$\begin{aligned} \frac{dP}{dI} = 0 \Leftrightarrow V + I\frac{dV}{dI} \approx V + I\frac{\Delta V}{\Delta I} = \\ = v(t) + i(t)\frac{v(t) - v(t-\Delta t)}{i(t) - i(t-\Delta t)} = 0 \end{aligned}$$
(13)

This MPPT deals with simple calculations only, which reduces expenses on the processing equipments.

The MPPT allows us to determine a control signal, S_P, that will enable us to control the photovoltaic panel in order to achieve the maximum power point, the relation between S_P and $\frac{dP}{dI}$ is defined in (14).

$$\begin{cases} \frac{dP}{dI} < 0 \rightarrow S_P = 0 \\ \frac{dP}{dI} = 0 \rightarrow S_P = 1 \\ \frac{dP}{dI} > 0 \rightarrow S_P = 2 \end{cases}$$
(14)

The control of $\frac{dP}{dI}$ cannot be made directly, it is only possible to control it by activating the switches of the matrix converter which means that we can only control $\frac{dI}{dt}$.

In Fig. 7 we can see the typical P-I relation, where P_{max} marks the maximum power point on the curve.

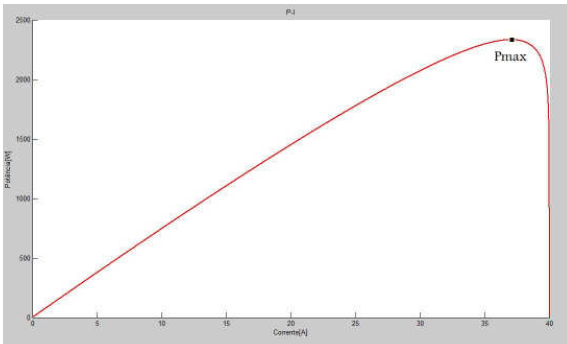

Fig. 7 – Typical P-I relation of a photovoltaic panel.

As we can see on Fig. 7, if $\frac{dP}{dI} < 0$ then we need $\frac{dI}{dt} > 0$ to reach P_{max}, and vice-versa.

If we consider the photovoltaic system as the source, which means the current flows from the photovoltaic system to the electric network, then to increase the current, I, we need to have $V_{DC} > V_{AC}$, and to decrease we need $V_{DC} < V_{AC}$. This means that the same vector can have different results, depending on the value of V_{AC} at that instant.

It becomes necessary to know the AC voltage value range. To do so we divided the voltage period of the composed network voltages in 12 zones with the same value ranges, Fig. 8.

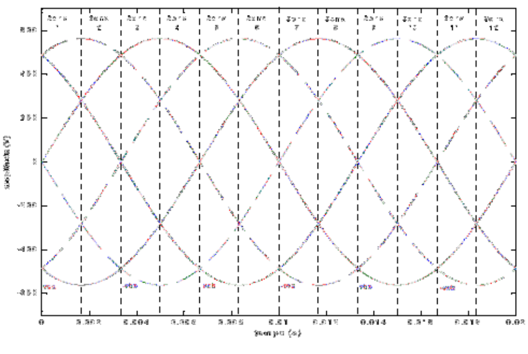

Fig. 8 – Voltage period division in 12 zones

Considering a photovoltaic panel with maximum voltage below 300V and the electric network of 230V, it is possible to create Table 3 with Fig. 8 and (14), where "x" represents the cases where it is impossible to determine the state vector effect because the AC voltage value can be either higher or lower than the DC voltage value.

Table 3 – Space vectors effect on the photovoltaic system output current, for each voltage zone

	Vector	1	2	3	4	5	6	7	8	9
	V_{DC}	V_{ab}	$-V_{ab}$	V_{bc}	$-V_{bc}$	$-V_{ca}$	V_{ca}	0	0	0
Zona de tensão	1	$\frac{dI_{bc}}{dt}<0$	$\frac{dI_{bc}}{dt}>0$	x	x	$\frac{dI_{bc}}{dt}<0$	$\frac{dI_{bc}}{dt}>0$	$\frac{dI_{bc}}{dt}>0$	$\frac{dI_{bc}}{dt}>0$	$\frac{dI_{bc}}{dt}>0$
	2	x	x	$\frac{dI_{bc}}{dt}<0$	$\frac{dI_{bc}}{dt}>0$	$\frac{dI_{bc}}{dt}<0$	$\frac{dI_{bc}}{dt}>0$	$\frac{dI_{bc}}{dt}>0$	$\frac{dI_{bc}}{dt}>0$	$\frac{dI_{bc}}{dt}>0$
	3	x	x	$\frac{dI_{bc}}{dt}<0$	$\frac{dI_{bc}}{dt}>0$	$\frac{dI_{bc}}{dt}<0$	$\frac{dI_{bc}}{dt}>0$	$\frac{dI_{bc}}{dt}>0$	$\frac{dI_{bc}}{dt}>0$	$\frac{dI_{bc}}{dt}>0$
	4	$\frac{dI_{bc}}{dt}>0$	$\frac{dI_{bc}}{dt}<0$	$\frac{dI_{bc}}{dt}<0$	$\frac{dI_{bc}}{dt}>0$	x	x	$\frac{dI_{bc}}{dt}>0$	$\frac{dI_{bc}}{dt}>0$	$\frac{dI_{bc}}{dt}>0$
	5	$\frac{dI_{bc}}{dt}>0$	$\frac{dI_{bc}}{dt}<0$	$\frac{dI_{bc}}{dt}<0$	$\frac{dI_{bc}}{dt}>0$	x	x	$\frac{dI_{bc}}{dt}>0$	$\frac{dI_{bc}}{dt}>0$	$\frac{dI_{bc}}{dt}>0$
	6	$\frac{dI_{bc}}{dt}>0$	$\frac{dI_{bc}}{dt}<0$	x	x	$\frac{dI_{bc}}{dt}>0$	$\frac{dI_{bc}}{dt}<0$	$\frac{dI_{bc}}{dt}>0$	$\frac{dI_{bc}}{dt}>0$	$\frac{dI_{bc}}{dt}>0$
	7	$\frac{dI_{bc}}{dt}>0$	$\frac{dI_{bc}}{dt}<0$	x	x	$\frac{dI_{bc}}{dt}>0$	$\frac{dI_{bc}}{dt}<0$	$\frac{dI_{bc}}{dt}>0$	$\frac{dI_{bc}}{dt}>0$	$\frac{dI_{bc}}{dt}>0$
	8	x	x	$\frac{dI_{bc}}{dt}>0$	$\frac{dI_{bc}}{dt}<0$	$\frac{dI_{bc}}{dt}>0$	$\frac{dI_{bc}}{dt}<0$	$\frac{dI_{bc}}{dt}>0$	$\frac{dI_{bc}}{dt}>0$	$\frac{dI_{bc}}{dt}>0$
	9	x	x	$\frac{dI_{bc}}{dt}>0$	$\frac{dI_{bc}}{dt}<0$	$\frac{dI_{bc}}{dt}>0$	$\frac{dI_{bc}}{dt}<0$	$\frac{dI_{bc}}{dt}>0$	$\frac{dI_{bc}}{dt}>0$	$\frac{dI_{bc}}{dt}>0$
	10	$\frac{dI_{bc}}{dt}<0$	$\frac{dI_{bc}}{dt}>0$	$\frac{dI_{bc}}{dt}>0$	$\frac{dI_{bc}}{dt}<0$	x	x	$\frac{dI_{bc}}{dt}>0$	$\frac{dI_{bc}}{dt}>0$	$\frac{dI_{bc}}{dt}>0$
	11	$\frac{dI_{bc}}{dt}<0$	$\frac{dI_{bc}}{dt}>0$	$\frac{dI_{bc}}{dt}>0$	$\frac{dI_{bc}}{dt}<0$	x	x	$\frac{dI_{bc}}{dt}>0$	$\frac{dI_{bc}}{dt}>0$	$\frac{dI_{bc}}{dt}>0$
	12	$\frac{dI_{bc}}{dt}<0$	$\frac{dI_{bc}}{dt}>0$	x	x	$\frac{dI_{bc}}{dt}<0$	$\frac{dI_{bc}}{dt}>0$	$\frac{dI_{bc}}{dt}>0$	$\frac{dI_{bc}}{dt}>0$	$\frac{dI_{bc}}{dt}>0$

For each voltage zone there is always more than one vector for each current operation.

With Table 3 we can now control the photovoltaic system to provide its maximum power.

4.2 Unitary power factor control

To guarantee unitary power factor we have to control the matrix converter output currents so that they are alternated sinusoidal and that they are in phase with the voltage.

To do so, we use the Blondel-Park transformation (15) on the α and β components of the output currents (16), [2].

$$\mathbf{P_B} = \begin{bmatrix} \cos\theta & \sin\theta & 0 \\ -\sin\theta & \cos\theta & 0 \\ 0 & 0 & 1 \end{bmatrix}$$

(15)

$$\begin{bmatrix} i_d \\ i_q \\ i_0 \end{bmatrix} = \mathbf{P_B} \begin{bmatrix} i_\alpha \\ i_\beta \\ i_0 \end{bmatrix}$$

(16)

The homopolar current, i_0, is null in both (d,q,0) and (α,β,0) systems. We can determine i_α and i_β with the Concordia transformation (17), [2].

$$\begin{bmatrix} i_\alpha \\ i_\beta \\ i_0 \end{bmatrix} = \mathbf{C}^\mathbf{T} \begin{bmatrix} i_a \\ i_b \\ i_c \end{bmatrix}$$

(17)

If we define the electric network voltages as (18) and consider θ = ωt then we can say that, to achieve unitary power factor, we need to have $i_q = 0$ [2].

$$\begin{cases} v_a = \sqrt{2} \times 230\cos(\omega t) \\ v_b = \sqrt{2} \times 230\cos(\omega t - 120^o) \\ v_c = \sqrt{2} \times 230\cos(\omega t - 240^o) \end{cases}$$

(18)

It is possible to represent the (d,q,0) current system in the α-β plane, however the representation will vary with the voltage zone, Fig. 9, [2].

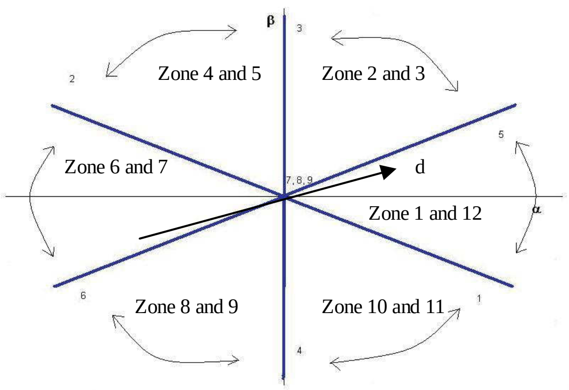

Fig. 9 – d axis location on the α-β plane for each voltage zone

The q axis will be orthogonal to the d axis, so we are also able to know the q axis location on the α-β plane for each voltage zone.

To have $i_q = 0$ we have to choose the space vector that will be nearest to the q axis.

Table 4 – Space vectors effect on the i_q current component, for each voltage zone

	Vector	1	2	3	4	5	6	7	8	9
	V_{DC}	V_{ab}	$-V_{ab}$	V_{bc}	$-V_{bc}$	$-V_{ca}$	V_{ca}	0	0	0
Zona de tensão	1	$\frac{diq}{dt}<0$	$\frac{diq}{dt}>0$	$\frac{diq}{dt}>0$	$\frac{diq}{dt}<0$	$\frac{diq}{dt}>0$	$\frac{diq}{dt}<0$	$\frac{diq}{dt}=0$	$\frac{diq}{dt}=0$	$\frac{diq}{dt}=0$
	2	$\frac{diq}{dt}<0$	$\frac{diq}{dt}>0$	$\frac{diq}{dt}>0$	$\frac{diq}{dt}<0$	$\frac{diq}{dt}<0$	$\frac{diq}{dt}>0$	$\frac{diq}{dt}=0$	$\frac{diq}{dt}=0$	$\frac{diq}{dt}=0$
	3	$\frac{diq}{dt}<0$	$\frac{diq}{dt}>0$	$\frac{diq}{dt}>0$	$\frac{diq}{dt}<0$	$\frac{diq}{dt}<0$	$\frac{diq}{dt}>0$	$\frac{diq}{dt}=0$	$\frac{diq}{dt}=0$	$\frac{diq}{dt}=0$
	4	$\frac{diq}{dt}<0$	$\frac{diq}{dt}>0$	$\frac{diq}{dt}<0$	$\frac{diq}{dt}>0$	$\frac{diq}{dt}<0$	$\frac{diq}{dt}>0$	$\frac{diq}{dt}=0$	$\frac{diq}{dt}=0$	$\frac{diq}{dt}=0$
	5	$\frac{diq}{dt}<0$	$\frac{diq}{dt}>0$	$\frac{diq}{dt}<0$	$\frac{diq}{dt}>0$	$\frac{diq}{dt}<0$	$\frac{diq}{dt}>0$	$\frac{diq}{dt}=0$	$\frac{diq}{dt}=0$	$\frac{diq}{dt}=0$
	6	$\frac{diq}{dt}>0$	$\frac{diq}{dt}<0$	$\frac{diq}{dt}<0$	$\frac{diq}{dt}>0$	$\frac{diq}{dt}<0$	$\frac{diq}{dt}>0$	$\frac{diq}{dt}=0$	$\frac{diq}{dt}=0$	$\frac{diq}{dt}=0$
	7	$\frac{diq}{dt}>0$	$\frac{diq}{dt}<0$	$\frac{diq}{dt}<0$	$\frac{diq}{dt}>0$	$\frac{diq}{dt}<0$	$\frac{diq}{dt}>0$	$\frac{diq}{dt}=0$	$\frac{diq}{dt}=0$	$\frac{diq}{dt}=0$
	8	$\frac{diq}{dt}>0$	$\frac{diq}{dt}<0$	$\frac{diq}{dt}<0$	$\frac{diq}{dt}>0$	$\frac{diq}{dt}>0$	$\frac{diq}{dt}<0$	$\frac{diq}{dt}=0$	$\frac{diq}{dt}=0$	$\frac{diq}{dt}=0$
	9	$\frac{diq}{dt}>0$	$\frac{diq}{dt}<0$	$\frac{diq}{dt}<0$	$\frac{diq}{dt}>0$	$\frac{diq}{dt}>0$	$\frac{diq}{dt}<0$	$\frac{diq}{dt}=0$	$\frac{diq}{dt}=0$	$\frac{diq}{dt}=0$
	10	$\frac{diq}{dt}>0$	$\frac{diq}{dt}<0$	$\frac{diq}{dt}>0$	$\frac{diq}{dt}<0$	$\frac{diq}{dt}>0$	$\frac{diq}{dt}<0$	$\frac{diq}{dt}=0$	$\frac{diq}{dt}=0$	$\frac{diq}{dt}=0$
	11	$\frac{diq}{dt}>0$	$\frac{diq}{dt}<0$	$\frac{diq}{dt}>0$	$\frac{diq}{dt}<0$	$\frac{diq}{dt}>0$	$\frac{diq}{dt}<0$	$\frac{diq}{dt}=0$	$\frac{diq}{dt}=0$	$\frac{diq}{dt}=0$
	12	$\frac{diq}{dt}<0$	$\frac{diq}{dt}>0$	$\frac{diq}{dt}>0$	$\frac{diq}{dt}<0$	$\frac{diq}{dt}>0$	$\frac{diq}{dt}<0$	$\frac{diq}{dt}=0$	$\frac{diq}{dt}=0$	$\frac{diq}{dt}=0$

We can define a control signal, S_Q, that enables us to control i_q. The relation between S_Q and i_q is (19).

$$\begin{cases} i_q < 0 \rightarrow S_Q = 0 \\ i_q = 0 \rightarrow S_Q = 1 \\ i_q > 0 \rightarrow S_Q = 2 \end{cases}$$

(19)

Both S_P and S_Q were determined using the slide mode control.

5 Simulation

The simulation model was developed in Matlab/Simulink, with resorting to the SimPowerSystems tool.

Many simulations were made using time-constant input data. For instance, with (20) where R_{on} is the equivalent switch conduction resistor.

$$\begin{aligned} & I_S = 40\,A \\ & m = 200 \\ & I_0 = 10^{-5}\,A \\ & V_T = 2{,}5 \times 10^{-2}\,V \\ & R_{on} = 20\,m\Omega \end{aligned}$$

(20)

We obtained (21).

$$\begin{aligned} & V_{DC} = 62{,}95\,V \\ & I_{DC} = 37{,}07\,A \\ & P_{DC} = 2334\,W \\ & I_{ACrms} = 3{,}14\,A \\ & P_{AC}\ 2168\,W \\ & \eta = 92{,}9\% \\ & THD = 2{,}9\% \end{aligned}$$

(21)

For this case, the input currents waveform are as showed in Fig. 10.

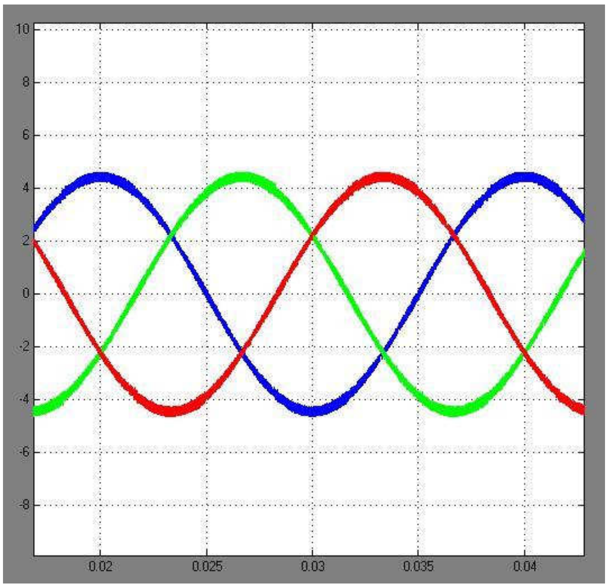

Fig. 10 – Electric network input currents waveform.

For obvious reasons, it was impossible to show all the simulation results.

The most important simulations, though, were made to emulate temperature and/or solar radiation variations along a simulation day.

5.1 Solar radiation variation

To simulate solar radiation variations we have to vary I_S, (5). The chosen I_S input signal is showed on Fig. 11 while the remaining values are equal to (20).

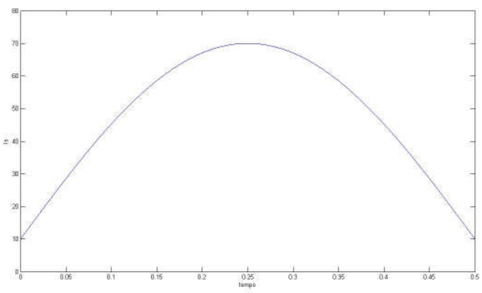

Fig. 11 – Input signal

The results are showed on Figs. 12 and 13.

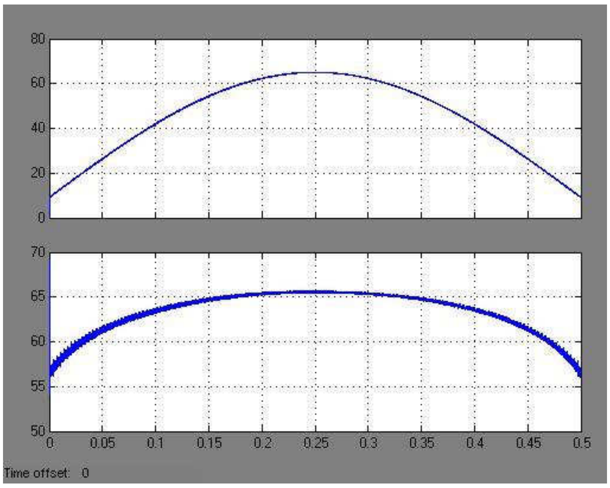

Fig. 12 – I_{DC}, up, and V_{DC}, down

In Fig. 12, the results are very similar to what was theoretically expected.

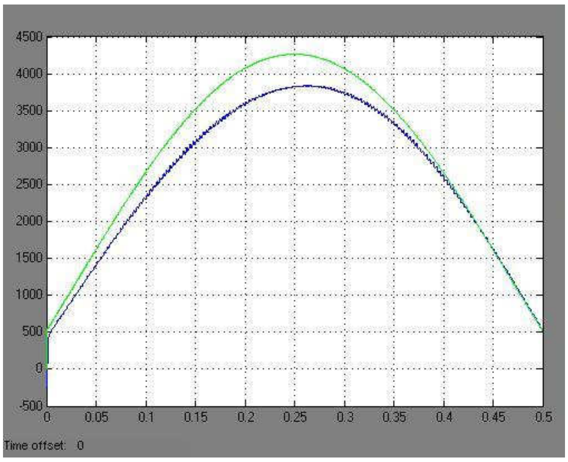

Fig. 13 – Photovoltaic system output power, pink, and electric network input power, yellow

In Fig. 13, we can watch the decrease of efficiency for higher solar radiation values.

Both figures show that this model has a behaviour similar to what would be expected in these situations, as previously showed in Fig. 4.

5.2 Temperature variation

To simulate temperature variation we have to vary both V_T and I_0, following (3) and (4). The chosen input signals are showed on Figs. 14 and 15 while the remaining values are equal to (20).

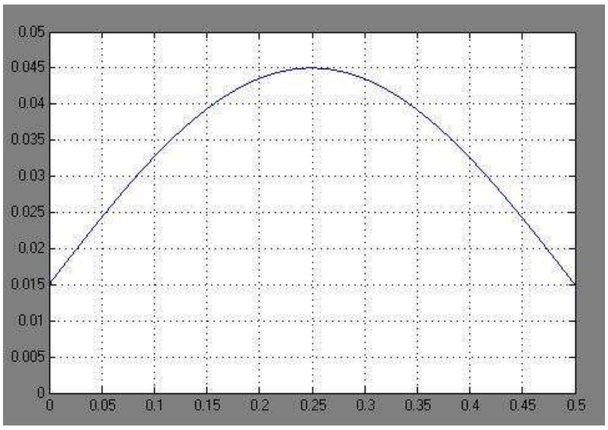

Fig. 14 –V_T input signal

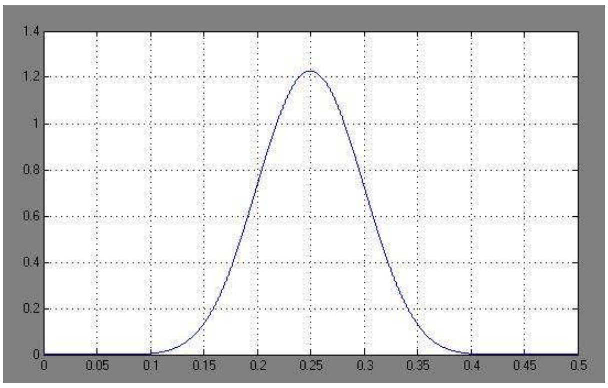

Fig. 15 – I_0 input signal

The results are showed on Figs. 16 and 17.

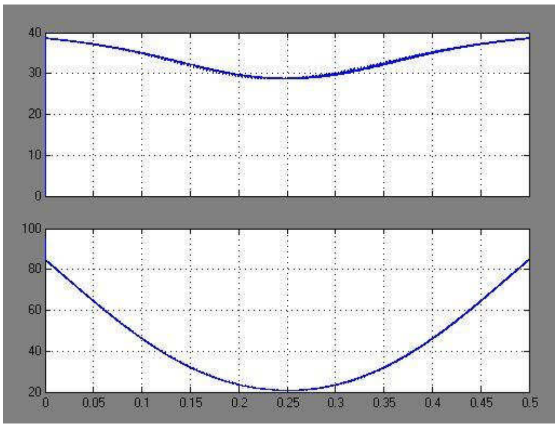

Fig. 16 – I_{DC}, up, and V_{DC}, down

In Fig. 16, the results are very similar to what was theoretically expected.

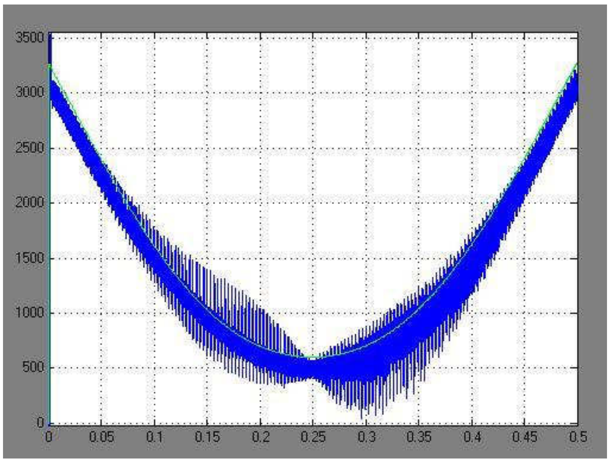

Fig. 17 – Photovoltaic system output power, pink, and electric network input power, yellow

In Fig. 17, we can watch that, although there is a decrease of efficiency for higher temperature values, it is much more slightest than what we could observe in Fig. 13.

There is much more signal distortion on Fig. 17 than on Fig. 13. In fact, temperature variations cause more dramatic V_{DC} variations which induces more distortion on the output currents.

Both figures show that this model has a behaviour similar to what would be expected in these situations, as previously showed in Fig. 3.

5.3 Temperature and solar radiation variation

This simulation pretends to demonstrate what would be the system behaviour during a standard day.

All values are equal to (20) except I_S, V_T and I_0. The input signals are showed on Figs. 18 and 19.

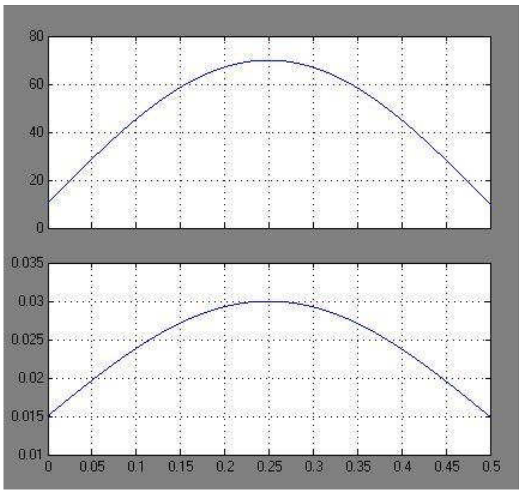

Fig. 18 – I_S, up, and V_T, down, input signals

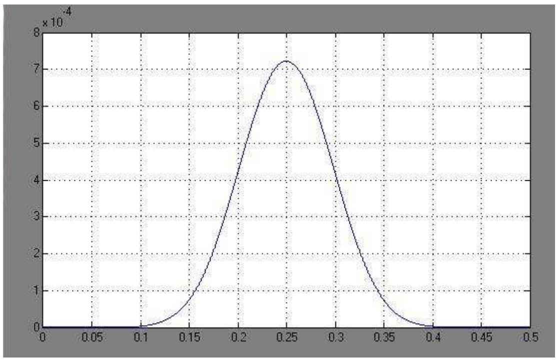

Fig. 19 – I_0 input signal

The results are showed on Figs. 20 and 21.

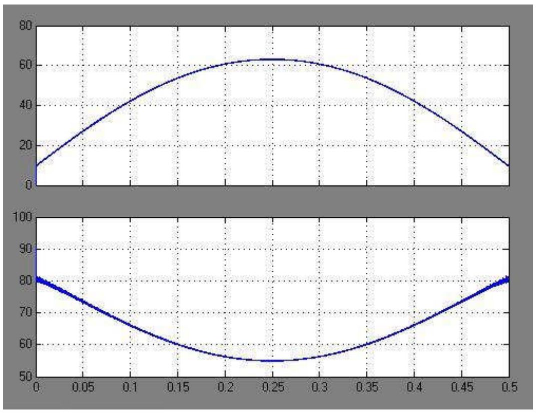

Fig. 20 – I_{DC}, up, and V_{DC}, down

In Fig. 20, we can see something like a crossing between Figs 12 and 16. With both strong current and voltage variation.

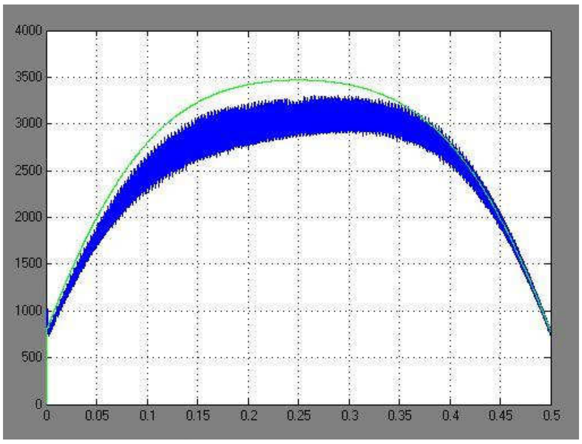

Fig. 21 – Photovoltaic system output power, pink, and electric network input power, yellow

In Fig. 21, also shows a crossing between Fig. 13 and Fig. 17. The system is more efficient that that on the first simulation but also has more signal distortion, due to stronger DC voltage variations. On the other hand, it is less efficient than the second simulation results, but has less distortion.

It is important to understand that, in these cases, power behaviour depends strongly on the system input values.

In Fig. 22 we can observe the power behaviour for different input values, same waveforms but different amplitudes.

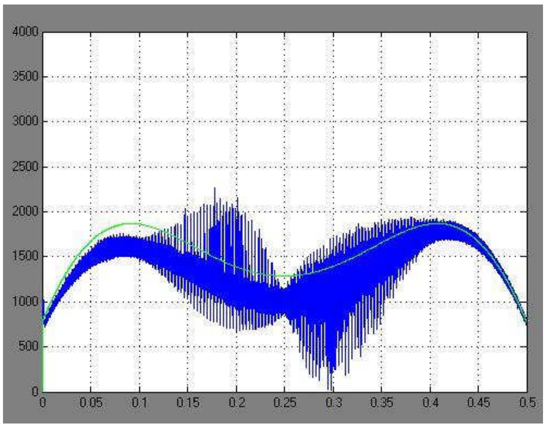

Fig. 22 – Photovoltaic system output power, pink, and electric network input power, yellow

We can still observe the crossing between Fig. 13 and Fig. 17, the system seems to be about as efficient as the first simulation and with about as much distortion.

But the major difference is the fact that the power waveform is not similar which makes it difficult to predict power behaviour in these cases.

6 Conclusions

By observation of the simulation results we can conclude that the simulation model is adequate to the study of the application of matrix converters in photovoltaic systems.

The result of the example time-constant input data simulation shows both good efficiency and harmonic distortion performance.

The results of time-variant input data simulations show good efficiency performance although we can see in some of these simulations some undesired harmonic distortion. However this can be rather easily eliminated resorting to additional filters.

The matrix converter appears to be a good alternative in these applications, not only for their good performance but also because of the advantages matrix converter technology bring, like the reduced size of the power converter. The biggest disadvantage is still the expensive cost of this solution.

7 Nomenclature

I_D Diode Current [A]

I_0 Dark Current [A]

m	Diode Ideality Factor	
V_T	Thermal Potential	[V]
V	Photovoltaic System Output Voltage	[V]
I	Photovoltaic System Output Current	[A]
I_S	Solar Radiation Generated Current	[A]
T	Absolute Temperature	[ºK]
T^r	Reference Absolute Temperature	(298,16ºK)
G	Solar Radiation	[W/m^2]
G^r	Reference Solar Radiation	(1000W/m^2)
K	Boltzmann's Constant	(1,3805x10^{-23}Nm/ºK)
q	Electron Charge	(1,6x10^{-19}C)
ε	Silicon Band Gap	(1,10eV)
V_T^r	Thermal Potential at T^r	[V]
I_0^r	Dark Current at T^r	[A]
I_S^r	Solar Radiation Generated Current at T^r	[A]
C	Concordia Transformation Matrix	
$\mathbf{P_B}$	Blondel-Park Transformation Matrix	
V_{DC}	Matrix Converter DC Input Voltage	[V]
I_{DC}	Matrix Converter DC Input Voltage	[A]
P_{DC}	Matrix Converter Input Power	[W]
R_{on}	Switch Conduction Resistor	[mΩ]
I_{ACrms}	Matrix Converter Output RMS Current	[A]
P_{AC}	Matrix Converter Output Power	[W]
η	Convertion Efficiency	[%]
THD	Total Harmonic Distortion	[%]

8 References

[1]. Santos, R., Honrado, D. Conversor Elevador Quadrático para Aproveitamento de Energia Renovavél. Instituto Superior Técnico, October 2006.

[2]. Menino, A., Antunes, J. Processamento Electricamente Não Poluente de Energia Eléctrica. Instituto Superior Técnico, July 2002.

[3]. Hosseini, S., Babaei, E. A Novel Modulation Method for DC/AC Matrix Converters Under Distorted DC Supply Voltage. Proceedings of IEEE TENCON'02, 2002, Pages 1970 – 1973.

[4]. Oyama, J., Higuchi, T., Abe, T, Matsuba, S., Teichmann, R. Application of ARCP Matrix Converter to AC/DC Conversion. IEEE PCC-Osaka, 2002, Pages 1061 – 1066.

[5]. Gil, R., Espí-Huerta, J., de la Calle, R., Maset, E., Castelló, J. Four-Quadrant AC/DC Matrix Converter with High-Frequency Isolation. IEE, 2004, Pages 515-520.

[6]. Ejea, J., Sanchis-Kilders, E., Carrasco, J., Espí, J., Ferreres, A. Implementation of Bi-Directional AC/DC Matrix Converter. Electronic Letters, Vol. 38, No. 16, August 1, 2002, Pages 933-934.

[7]. Castro, R. Introdução à Energia Fotovoltaica. Instituto Superior Técnico, 2nd Edition, May, 2007.